Subunits of the Yeast Mitochondrial ADP/ATP Carrier: Cooperation within the Dimer†

Vincent Postis, Carine De Marcos Lousa,‡ Bertrand Arnou, Guy J.-M. Lauquin, and Véronique Trézéguet*

Laboratoire de Physiologie Moléculaire et Cellulaire, UMR 5095-Université de Bordeaux2-CNRS, IBGC, 1, rue Camille Saint-Saëns, 33077 Bordeaux Cedex, France

Received August 18, 2005; Revised Manuscript Received September 20, 2005

ABSTRACT: The mitochondrial ADP/ATP carrier, or Ancp, is a member of the mitochondrial carrier family (MCF). It exchanges ADP and ATP between matrix and intermembrane space. It is postulated from numerous experiments that the inactive Ancp bound to one of its inhibitors (CATR or BA) is a dimer, and it is inferred that the active unit is a dimer, too. However, the structure of beef Ancp bound to CATR obtained at high resolution is that of a monomer. To ascertain the dimeric organization of Ancp, we have constructed covalent tandem dimers of which one "subunit" (protomer) is the wild type and the other is inactive for ADP/ATP exchange. We have chosen either the *op1* mutant or another member of the MCF, the phosphate carrier (Picp). Activities of the chimeras were first evaluated in vivo. The Ancp/op1 constructs exchange the adenine nucleotides. The Anc/Pic chimeras are considered as bifunctional forms since they exchange ADP and ATP and transport P_i within the same cells. We have then controlled the fact that the chimeras are stable in vivo and in vitro. Proteinase K digestion showed that both protomers of Ancp/op1 have similar organization in the membrane. Analyses of kinetic properties indicated that protomers of Ancp/op1 chimeras crosstalk during the nucleotide exchange unlike those of Anc/Pic. However, full inhibition of phosphate uptake by CATR, a very specific inhibitor of Ancp, strongly suggests that the native functional unit of Ancp, and thus of Picp, is a dimer.

Mitochondrial carriers make up a family of integral transporters (MCF)[1] embedded in the mitochondrial inner membrane (MIM) that allow fluxes of metabolites between the matrix and cytoplasm. Two members play an important energetic role, the phosphate carrier (Picp) and the ADP/ATP carrier (Ancp). They supply ATP synthase with its substrates, ADP and inorganic phosphate (P_i), and Ancp replenishes the cytosol with ATP, which fuels most of the metabolic processes in the cell. Ancp is one of the most abundant proteins of the MIM and has been studied for a long period of time. Since members of MCF share structural properties, Ancp is used as a model to help in the deciphering of properties of mitochondrial carriers.

Recently, the three-dimensional structure of Ancp was the first to be unraveled at high resolution (*1*). The structure is one of a six-transmembrane helix bundle, tightly closed on the matrix side and widely open toward the intermembrane space. Analyses of residues located in the cavity hint at the mechanism of nucleotide binding and translocation. However, the crystal unit cell contains one monomer per asymmetric unit, and there is no indication of dimerization of the carrier (*1*). This was puzzling since Ancp was crystallized in the presence of carboxyatractyloside (CATR), a powerful inhibitor of Ancp, and it was inferred from several experimental approaches that Ancp bound to CATR is a dimer (*2*−*5*). Moreover, kinetic analyses led to the assumption that the functional unit is at least a dimer (*6*). Such a dimeric organization was also inferred for Picp from reconstitution experiments (*7*). Although oligomeric organization can persist during the crystallization process, extensive detergent use during Ancp purification may explain oligomer disruption.

Nevertheless, X-ray data allow us to rule out the possibility that the monomer interface constitutes the CATR binding site and the nucleotide pathway. Those are rather located in the cavity shaped by the six transmembrane helices of Ancp. Considering that Ancp exchanges adenine nucleotides with a strict stoichiometry of 1:1, one can suppose that two monomers will cooperate to transport ADP and ATP.

In this work, crosstalk between the two subunits of Ancp is investigated within the frame of a covalent tandem dimer of *Saccharomyces cerevisiae* Anc2p [$(Anc2p)_2$] that was shown to exhibit kinetic properties similar to those of the

† This work was supported by the University of Bordeaux2, the Centre National de la Recherche Scientifique, and the Région Aquitaine. V.P. was supported by the French Ministère de la Recherche et de la Technologie.

* To whom correspondence should be addressed. E-mail: vero.trezeguet@ibgc.u-bordeaux2.fr. Phone: (33) 556 99 90 39. Fax: (33) 556 99 90 63.

‡ Present address: Institute of Molecular Biology and Biotechnology, FORTH, P.O. Box 1527 Vassilika Vouton, 71110 Heraklion, Crete, Greece.

[1] Abbreviations: Ancp, mitochondrial ADP/ATP (adenine nucleotide) carrier protein; *ANC*, mitochondrial ADP/ATP carrier encoding gene; ATR, atractyloside; B, bovine; BA, bongkrekic acid; CATR, carboxyatractyloside; IMS, mitochondrial intermembrane space; MCF, mitochondrial carrier family; MIM, mitochondrial inner membrane; D_x, attenuance at x nm; P_i, inorganic phosphate; Pic, mitochondrial phosphate carrier; *PIC* and *MIR1*, mitochondrial phosphate carrier encoding gene; PK, proteinase K; Sc, *S. cerevisiae*; SDS−PAGE, sodium dodecyl sulfate−polyacrylamide gel electrophoresis; TMS, transmembrane segment; YPD, rich yeast extract peptone dextrose medium.

10.1021/bi051648x CCC: $30.25
Published on Web 10/19/2005

wild-type *S. cerevisiae* Anc2p (*8*). We constructed chimeras in which one of the two "subunits", named protomers, is of the wild type and the other one is inactive for the adenine nucleotide transport. It corresponded either to the Sc Anc2p *op1* mutant (*9*) or to Picp which cannot exchange ADP and ATP. Picp belongs to MCF and as such is supposed to be folded in a manner similar to that of Ancp. Four different chimeras were created: Anc2-op1p and op1-Anc2p (Ancp/op1 chimeras) and Anc2-Picp and Pic-Anc2p (Anc/Pic chimeras). The *op1* mutation changes R96 of Anc2p into H96 (*10*). It was chosen because the yeast strain which carries this mutation is unable to develop on a nonfermentable carbon source, such as glycerol or lactate, for more than two generations (*9*). However, the amount of op1p in MIM is equivalent to that of wild-type Anc2p (*11*). This is not the case for most inactive Anc2p mutants, which are usually present in much smaller amounts (*12*).

All of the heterochimeras, Anc2/op1 or Anc2/Pic, were functional in vivo and catalyzed the ADP/ATP exchange in isolated mitochondria. Furthermore, the Anc2/Pic chimeras were bifunctional since they ensured growth on a nonfermentable carbon source of a yeast strain inactivated for both Picp and Anc2p functions.

Folding of the Anc2/op1 chimeras in MIM was studied by limited proteinase K digestion. Kinetic properties of the four chimeras, atractylate binding and nucleotide exchange, were determined with isolated mitochondria. Extensive analyses of the results allowed to suggest that both monomers of Anc2p fold in a similar way and that they cooperate during nucleotide transport. Furthermore, Anc2/Pic heterochimera properties support the idea that the functional forms of the adenine nucleotide carrier and of the phosphate carrier are dimers.

MATERIALS AND METHODS

Construction of the Yeast Strain Inactivated for the Mitochondrial ADP/ATP and Phosphate Carriers, Δpic Δanc2. The mitochondrial phosphate carrier-encoding gene was formerly named *MIR1*. The *MIR1*-disrupted strain of *S. cerevisiae*, Δ*pic* (*MAT*α, *ade2-1, leu2-3,112, his3-11,15, trp1-1, can1-100, ura3-1, mir1::LEU2*), was a gift from N. Pfanner (*13*). Δ*pic* was crossed with Δ*anc2* (*MATa ade2-1, leu2-3,112, his3-11,15, trp1-1, can1-100, ura3-1, anc2::URA3*) (V. Trézéguet, unpublished data). The resulting spores that were URA^+ and LEU^+ were selected, and their auxotrophies were controlled by growth on the appropriate media. A spore that was LEU^+, URA^+, and $glycerol^-$ was further isolated and named Δ*anc2*Δ*pic* (*MATa ade2-1 leu2-3,112 his3-11,15 trp1-1 can1-100 ura3-1, mir1::LEU2 anc2::URA3*). Inactivations of *ANC2* and *MIR1* genes were controlled by PCR amplification and sequencing.

Other Strains, Media, and Transformation. The *Escherichia coli* strain used for plasmid propagation was XL1-Blue {*recA1 endA1 gyrA96 (Nal^r) thi hsdR17 (r_K^- m_K^+) supE44 relA1 lac$^-$ F′ [Tn10 (tet^r) proAB$^+$ lacI^q lacZΔM15]*}. Bacteria were transformed according to standard methods either with calcium chloride (*7*) or by electroporation. The following *S. cerevisiae* strains were used in this study: *JL1-3* (*MAT*α *leu2-3,112 his3-11,15 ade2-1 trp1-1 ura3-1 can1-100 anc1::LEU2 anc2::HIS3 anc3::URA3*) (*14*), *JL1-3Δ2* (*MAT*α *leu2-3,112 his3-11,15 ade2-1 trp1-1 ura3-1 can1-100 anc1::LEU2* Δ*anc2::HIS3 anc3::URA3*) (*15*), and *JL1-3ANC2* (*MAT*α *leu2-3,112 his3-11,15 ade2-1 trp1-1 ura3-1 can1-100 anc1::LEU2 anc3::URA3*) which refers to the *2N1-3* strain (*16*). The strains were cultivated as described in ref *6*. Yeast transformation was carried out by the lithium chloride method (*8*).

Chemicals. [^{3}H]Atractyloside (ATR) was synthesized as previously described (*17*). Protein concentration was determined using the bicinchoninic acid reagent kit from Sigma. Nucleotides and CATR were purchased from Sigma, and P^1,P^5-di(adenosine-5′)-pentaphosphate was from Calbiochem. Hexokinase/glucose-6-phosphate dehydrogenase enzyme mix and proteinase K were obtained from Roche Diagnostics GmbH.

Cloning of Covalent Tandem Heterodimers. A *Kpn*I−*Sal*I fragment (2.8 kb) containing *anc2* with the *op1* mutation and the 5′- and 3′-flanking DNA regions (G. Lauquin, unpublished data) was introduced into the centromeric plasmid pRS314 (*18*). The resulting plasmid is pRSop1. A *Bsp*MI−*Bsp*MI fragment of the *op1* ORF, which contains the *op1* mutation, was exchanged with the *Bsp*MI−*Bsp*MI fragment of *anc2* in KSanc2fus5′3′ or KSANC2(*Bam*HI) (*8*) to obtain KSfop15′3′ or KSop1(*Bam*HI), respectively. The *ANC2* and *op1* genes, flanked by two *Bam*HI sites, were obtained by *Bam*HI digestion of KSANC2(*Bam*HI) and KSop1(*Bam*HI), respectively, and were ligated in KSfop15′3′ and KSanc2fus5′3′, respectively. The resulting plasmids were KSfop1-ANC25′3′ and KSfus-op15′3′. The *Kpn*I−*Sac*I fragments (4.4 kb) containing the *ANC2-op1* and *op1-ANC2* genes and the 5′- and 3′-flanking regions of *ScANC2* were used to transform the *JL1-3* strain or were subcloned into the pRS314 phagemid. Correct integration in yeast at the *ScANC2* chromosomal locus was controlled by Southern blot analyses. The resulting strains were named *ANC2-op1* or *op1-ANC2* and the resulting plasmids pRS(ANC2-op1) and pRS(op1-ANC2). The *ANC2* fragment was then replaced with *op1* in pRS(ANC2-op1) to generate the $pRS(op1)_2$ plasmid.

The *PIC* ORF (*MIR1* gene) without the stop codon, named *PUS(MI/BI)*, was PCR amplified with *Pfu* DNA polymerase (Promega) and the following primers: 5′-caattgATGTCTGTGTCTGCTGCTCCTGC (*Mfe*I site in lowercase letters) and 5′-ggatccATGACCACCACCACCAATTTC (*Bam*HI site in lowercase letters), using *JL1-3* genomic DNA as the matrix. The *PIC* ORF was amplified using the following primers: 5′-ggatccATGTCTGTGTCTGCTGCTCCTGC (*Bam*HI site in lowercase letters) and 5′-agatctCTAATGACCACCACCACCAATTTC (*Bgl*II site in lowercase letters). The PCR fragments were subcloned in pGEM-T (Promega). They were exchanged with *anc2* fragments of pRSDIM5′3′ (*8*) to obtain pRS(PIC-ANC2) and pRS(ANC2-PIC). The sequences of the open reading frames of these chimeras were controlled by DNA sequencing (ABI PRISM 310, Applied Biosystems). The fragments containing *ANC2-PIC* or *PIC-ANC2* flanked by the 5′- and 3′-noncoding regions were introduced at the *anc2* locus of Δ*anc2*Δ*pic*. The resulting strain was named *ANC2-PIC* or *PIC-ANC2*, respectively.

Limited Proteinase K Proteolysis of Mitoplasts. Mitoplasts were obtained by osmotic swelling of mitochondria incubated for 15 min on ice in 9 volumes of 10 mM Tris-HCl (pH 7.4). After addition of 40 volumes of 0.6 M mannitol and 50 mM MOPS (pH 6.8) and a 15 min incubation on ice,

mitoplasts were pelleted at 48000*g* for 10 min. They were then resuspended (1 mg of protein/mL) in 0.6 M mannitol and 50 mM MOPS (pH 6.8). Proteinase K (PK) digestion was performed at 25 °C with different proteinase K:mitoplast protein ratios [1:50 (w/w) or 1:10 (w/w)]. Digestion was stopped by addition of PMSF (final concentration of 1 mM).

Swelling of Mitochondria. Mitochondria (0.2 mg) were incubated for 3 min in 200 μL of 0.6 M mannitol, 10 mM Tris-HCl (pH 7.4), and 0.1 mM EGTA supplemented with 0.5 μg of oligomycin, 0.5 μg of antimycin A, and 1 μM FCCP. Mitochondria were then diluted in 960 μL of 240 mM potassium phosphate (pH 6.8). Swelling was monitored by measuring the attenuance decrease at a λ of 500 nm after valinomycin addition (0.4 μg/mg of protein). Mersalyl (125 nmol/mg of protein) and CATR (1.25 nmol/mg of protein) were added where indicated.

Other Methods. The protocols and materials used to perform isolation of mitochondria, ADP/ATP transport, [^{3}H]-ATR binding measurements, and protein immunostaining are described in ref *15*. To prevent protein degradation during isolation of mitochondria, a cocktail of protease inhibitors was added to the homogenization and resuspension buffers: pepstatin A (1 μg/mL), leupeptin (1 μg/mL), antipain (1 μg/mL), aprotinin (5 μg/mL), and EDTA (1 mM).

RESULTS

Anc2/op1 and Anc2/Pic Chimeras Are Functional in Vivo. Four covalent heterodimer genes were constructed with the same strategy that was used for the (*ANC2*)$_2$ gene (*8*). The resulting genes are expected to produce pseudodimeric proteins in which the two "subunits" are named protomers. Those are covalently linked by a glycine followed with a serine, and are not functionally equivalent: one is active for the ADP/ATP exchange and the other not. The inactive protomer (op1 or Pic) was either upstream or downstream of the active protomer (Anc2).

Functions of the Anc2/op1 and Anc2/Pic chimeras were examined in a *S. cerevisiae* strain, *JL1-3*Δ*2*, in which the three *ANC* genes were inactivated (*15*). Functions of the Anc2/Pic chimeras were also evaluated in two *S. cerevisiae* strains of which the mitochondrial phosphate carrier encoding gene (*MIR1*) was inactivated alone, Δ*pic*, or in combination with *ANC2*, Δ*anc2*Δ*pic* (see Materials and Methods). None of the three strains can grow in the presence of glycerol or lactate as the sole carbon source. Growth of their transformants on YPLact plates is thus a good indication of gene product function.

As can be seen in Figure 1, *JL1-3*Δ*2* cells transformed with pRSop1 or pRS(op1)$_2$ are unable to develop on YPLact. On the other hand, *ANC2-op1* and *op1-ANC2* genes restored a very efficient growth of *JL1-3*Δ*2* cells (Figure 1). Similarly, Δ*anc2*Δ*pic* cells could not develop on YPLact at 28 °C, but the *ANC2-PIC* or *PIC-ANC2* gene restored very efficient growth under the same conditions. Therefore, the four chimera genes all encode proteins that can exchange adenine nucleotides. The growth doubling times in liquid lactate medium were either similar or increased 1.4−1.8 times compared to those of the wild-type strains (Figure 1). The *ANC2-PIC* and *PIC-ANC2* genes allowed both strains inactivated for *MIR1*, Δ*pic* (data not shown) and Δ*pic*Δ*anc2*, to grow on lactate (Figure 1). Thus those two genes can

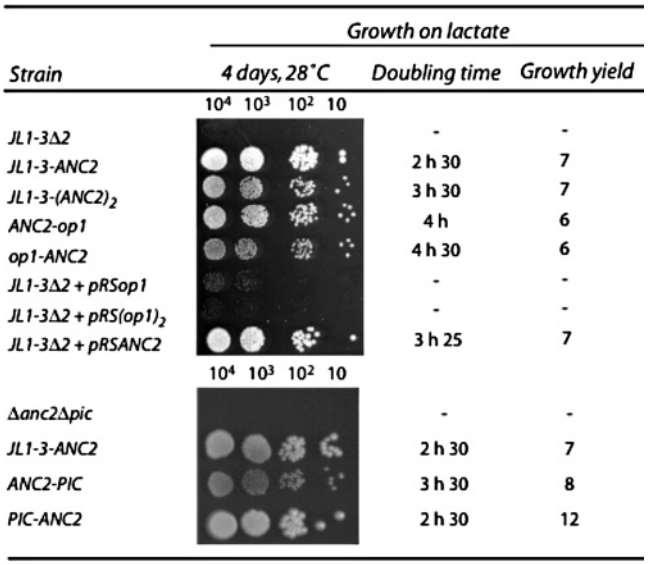

FIGURE 1: Covalent heterochimeras allow yeast growth on a nonfermentable carbon source. Cultures of yeast cells were diluted and plated (10^4−10^2 cells) onto a rich medium containing lactate (YPLact). Plates were incubated for 4 days at 28 °C. Growth yields and doubling times were determined from liquid cultures at 28 °C in liquid YPLact, for which D_{600} was measured at different time intervals. Growth yields correspond to the values of D_{600} measured during the stationary phase of cultures.

complement simultaneously *anc* and *pic* inactivations and as a consequence produce in the same cell functional Ancp and functional Picp.

Carriers Translated from Chimera Genes Are Covalent Tandem Dimers. Growths observed above could have arisen from wild-type Anc2p and/or Picp activities resulting from in vivo proteolysis of chimera gene products. This hypothesis was ruled out by immunostaining of cell extracts with an antibody recognizing the 14 C-terminal amino acids of Anc2p (*19*). In *JL1-3ANC2* cell extract, the antibody recognized a protein migrating at the same position as the wild-type Anc2p (32 kDa) (Figure 2A). Cell extracts from *ANC2-op1*, *op1-ANC2*, and *JL1-3*(*ANC2*)$_2$ were prepared from cells grown in lactate-containing medium. The antibody recognized mainly a protein with an apparent size of 64 kDa. This size corresponds to twice that of the wild-type Anc2p, and thus to a covalent tandem dimer of this carrier (Figure 2A). This was also the case when cells were grown in galactose-containing medium (YPGal) (data not shown) prior to cell extract preparation. A similar result was obtained with *JL1-3*Δ*2* transformed with pRSop1-op1 and grown in galactose-containing medium (YPGal). This indicated that though inactive the covalent tandem dimer of op1p is stable and can be used as a reference for further studies.

In the cases of *ANC2-PIC* and *PIC-ANC2*, the size of the chimera gene products corresponded to the sum of Picp and Anc2p sizes (Figure 2B). In the Δ*pic* strain, a 32 kDa protein was also detected that could be attributed to the endogenous Anc2p protein, the gene of which was not inactivated in this strain. As will be discussed later, the interconnecting region between two protomers of a covalent tandem dimer is readily proteolyzed. In the case of Anc2/Pic heterochimeras, such a proteolysis would have generated two proteins of ∼30 and ∼32 kDa, corresponding to Anc2p and Picp, respectively, yet no protein of this size was detected in the Δ*anc2*Δ*pic* cells with antibodies raised against Picp (data not shown)

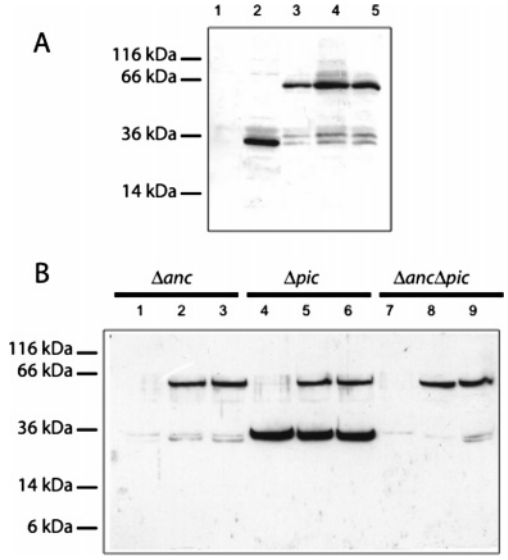

FIGURE 2: Carriers produced from chimera genes are covalent tandem dimers. (A) Cell extracts were prepared from 1.5 unit D_{600} of *JL1-3Δ2* (1), *JL1-3-ANC2* (2), *JL1-3-(ANC2)$_2$* (3), *ANC2-op1* (4), and *op1-ANC2* (5). Cells were cultivated in YPGal (1) or YPLact (2−4). After SDS−PAGE, proteins were transferred onto a nitrocellulose filter and immunostained with an antibody directed against the whole Anc2p. (B) Extracts were prepared from *JL1-3Δ2* (1−3), Δ*pic* (4−6), and Δ*anc*Δ*pic* (7−9) cells not transformed (1, 4, and 5) or transformed with pRS(ANC2-PIC) (2, 5, and 8) or pRS(PIC-ANC2) (3, 6, and 9). Nontransformed cells were grown in YPGal and transformed cells in YPLact. After SDS−PAGE, proteins were transferred onto a nitrocellulose filter and immunostained with an antibody directed against whole Anc2p.

or Anc2p C-ter (Figure 2B). Therefore, Pic-Anc2p and Anc2-Picp are bifunctional covalent heterodimers that exchange ADP/ATP and transport P_i. Those two activities could be catalyzed simultaneously or alternatively by the same heterochimera molecule or independently by two chimera molecules within the same cell.

Prior to characterizing the properties of heterochimeras, we have examined their stability in isolated mitochondria. Partial proteolysis occurred during isolation (data not shown) which was overcome by adding to the preparation buffers a protease inhibitor cocktail (1 μg/mL pepstatin A, 1 μg/mL leupeptin, 1 μg/mL antipain, 5 μg/mL aprotinin, and 1 mM EDTA) that was used in previous studies of the $(Anc2p)_2$ covalent tandem dimer (*8*).

Heterochimeras Bind Atractyloside, a Specific Inhibitor of Ancp. ATR is a very specific inhibitor of Ancp, and it was inferred from several experimental approaches that the binding stoichiometry of ATR to Ancp is 1:2 (*2*−*5*). In addition, because of its high specificity and affinity for Ancp, the maximum number of [^{3}H]ATR-binding sites (ATR_{Max}) allows us to quantify the amount of Ancp present in the membrane. Results of [^{3}H]ATR binding experiments with isolated mitochondria are given in Table 1. Interestingly, ATR bound to op1p and to all covalent chimeras, indicating that the presence of an inactive protomer covalently linked to Anc2 did not preclude ATR binding. In addition, ATR affinity was a little better for all the Anc2/op1 variants than for wild-type Anc2p. As expected, in the case of wild-type Anc2p, the ATR_{Max} value was higher when mitochondria were isolated from cells grown in lactate than in galactose-containing medium. Under both conditions, ATR_{Max} values for the covalent tandem dimer $(Anc2p)_2$ and for op1p were

Table 1: Kinetic Parameters of Binding of [^{3}H]ATR to Isolated Mitochondria[a]

Anc2p variant	ATR_{Max} (pmol/mg of protein)[b]	K_d^{ATR} (nM)[b]
Anc2p[c]	337 ± 27	327 ± 26
$(Anc2p)_2$[c]	389 ± 45	164 ± 95
Anc2-op1p[c]	205 ± 53	125 ± 3
op1-Anc2p[c]	231 ± 8	187 ± 93
op1p[c]	445 ± 236	226 ± 116
$(op1p)_2$[c]	190 ± 110	130 ± 25
Anc2p[d]	594 ± 41	415 ± 78
$(Anc2p)_2$[d]	537 ± 5	362 ± 42
Anc2-Picp[d]	329 ± 9	334 ± 102
Pic-Anc2p[d]	369 ± 1	99 ± 14

[a] [^{3}H]ATR binding was assessed with isolated mitochondria. [b] The values are the means of at least three determinations. [c] Cells were cultivated in galactose-containing medium. [d] Cells were cultivated in lactate-containing medium.

in the same range as that of Anc2p. However, the covalent tandem dimers $(op1p)_2$, Anc2-op1p, and op1-Anc2p bound ATR roughly 2 times less efficiently (Table 1). This was also the case for the Anc2/Pic heterochimeras. Such differences could reflect an improper insertion of one of the protomers of the covalent dimers in MIM, thus precluding effective ATR binding.

Anc2/op1 Heterodimers Are Properly Embedded within the Membrane. Though improper folding is not very likely because K_d^{ATR} values reflect similar or even better affinities for the variants than for Anc2p, we have examined this possibility with limited proteolysis experiments. We noticed that during isolation of mitochondria in the absence of protease inhibitors, the covalent tandem dimers (62 kDa) were split, giving rise on SDS−PAGE to a band at ∼30 kDa immunostained with a specific antibody raised against Anc2p C-ter. We attributed this phenomenom to a "monomerization" process, explained by the high sensitivity to proteases of the artificial interconnecting loop between two protomers. Addition of low concentrations of PK to mitoplasts (1:50, w/w) induced the same monomerization process, and the resulting 30 kDa protein was stable over the time. It was thus possible to quantify the amount of Anc2p epitope in mitochondria before and after addition of PK.

If one of the protomers of a covalent tandem dimer was not inserted in MIM, it would be quite accessible to the protease and thus degraded. The resulting amount of the Anc2p epitope detected around the ∼30 kDa position would represent 50% of the initial amount of the Anc2p epitope at 62 kDa. As can be seen in Table 2, for an efficient monomerization of covalent dimers (80−100%), the epitope recoveries largely exceeded 50%: 79% for $(Anc2p)_2$, 95% for Anc2-op1p, and 99% for op1-Anc2p. These results indicated that both protomers of the covalent homo- and heterodimers were inserted in MIM and thus protected from PK degradation.

A higher PK:mitoplast protein ratio (1:10, w/w) led to partial digestion of Anc2p in three characteristic bands on SDS−PAGE stained with the anti-Anc2p C-ter antibody (Figure 3). The sizes of these fragments were compatible with cleavages in the cytosolic loops, and they were not observed when Anc2p was first solubilized in Triton X-100 (Figure 3). We can thus infer that this proteolysis pattern accounts for a proper Anc2p membrane insertion. Degradation of the three covalent dimers $(Anc2p)_2$, Anc2-op1p, and

Table 2: Conservation of the Amount of Anc2p Epitope during Proteolytic Monomerization of Various Covalent Dimers[a]

covalent dimer	monomerization (%)[b]	epitope recovery (%)[c]
$(Anc2p)_2$	80	79
Anc2-op1p	100	95
op1-Anc2p	100	99

[a] Mitoplasts were incubated with proteinase K (1 μg/50 μg of mitochondrial proteins) for 30 min at 25 °C. Proteolysis was stopped with PMSF, and mitoplast proteins were subjected to SDS−PAGE. After being transferred onto a nitrocellulose membrane, proteins were immunostained with an antibody directed against a peptide corresponding to the last 14 amino acids of Anc2p. The signal obtained after incubation with the secondary antibody was quantified by densitometry. [b] The monomerization percent corresponds to the ratio of the signal intensity at 30 kDa after proteolysis to the initial signal intensity at 62 kDa (before PK digestion). [c] The epitope recovery corresponds to the ratio of the sum of the signal intensities after proteolysis (62 and 30 kDa) to the initial signal intensity before proteolysis (62 kDa).

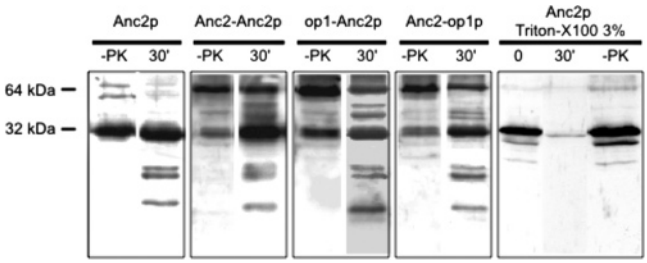

FIGURE 3: Anc2/op1 heterodimers are properly embedded within MIM. Mitoplasts were incubated with proteinase K (10:1, w/w) for 30 min at 25 °C. Proteolysis was stopped by adding PMSF (1 mM). After SDS−PAGE of mitoplasts (10 μg) before (−PK) and after (+PK) addition of PK, proteins were transferred onto a nitrocellulose membrane and stained with an antibody raised against the final 14 amino acids of Anc2p. The two panels on the right side correspond to analysis of Anc2p mitoplats solubilized in 50 mM Na_2SO_4 and 3% Triton X-100 (detergent:protein ratio, w/w) before (−PK) or after (0 and 30 min) addition of proteinase K (1 mg/50 mg of mitoplast proteins).

op1-Anc2p led to the appearance of the monomerization fragment (30 kDa) and of three additional peptides, the migration patterns of which were similar to that of Anc2p peptides (Figure 3). We can therefore conclude that, whatever the covalent dimer, the wild-type and op1 protomer insertions in MIM are equivalent.

Anc2/op1 Protomers Cooperate during ADP/ATP Exchange. We have determined the kinetic parameters of cytosolic ADP versus matrix ATP exchange for the two Anc2/op1 heterodimers in isolated mitochondria and compared them to those of Anc2p and $(Anc2p)_2$. Variation of the exchange rate as a function of free ADP concentration was examined as described in ref *15*. op1p and op1-op1p were examined as controls, but since these proteins cannot confer cell growth in lactate medium, all the cells producing Anc2p, op1p, homodimers, and Anc2/op1 heterodimers were grown in galactose-containing medium prior to isolation of mitochondria. As can be seen in Table 3, the maximum exchange rate values, V_{max}^{ADP}, do not vary with the Anc2p variant, but the *op1* mutation modifies dramatically the Michaelis constant for externally added ADP, K_M^{ADP}. The value increases from 0.68 μM for wild-type Anc2p to 368 μM for op1p and 574 μM for $(op1p)_2$. The presence of the covalent link between two protomers has a much weaker effect than the *op1* mutation since it increased only

Table 3: Kinetic Parameters of ADP/ATP Exchange in Isolated Yeast Mitochondria[a]

protein	K_M^{ADP} (μM)[b]	V_{max}^{ADP} (nmol min^{-1} mg^{-1})[b]
Anc2p[c]	0.68 ± 0.08	90 ± 2.6
op1p[c]	368 ± 66	93.6 ± 7.8
$(Anc2p)_2$[c]	2.3 ± 0.29	90.6 ± 2.2
Anc2-op1p[c]	41.2 ± 4.9	82 ± 2.9
op1-Anc2p[c]	33.4 ± 3.7	87.5 ± 2.9
$(op1p)_2$[c]	574 ± 150	129 ± 20
Anc2p[d]	0.92 ± 0.09	99 ± 7
Anc2-Picp[d]	6.6 ± 3.1	108 ± 2
Pic-Anc2p[d]	1.9 ± 0.4	118 ± 5.8

[a] Kinetic parameters of ADP/ATP exchange in isolated yeast mitochondria were measured as described in ref *15*. [b] The given values are the averages of at least two independent experiments. [c] Cells were cultivated in galactose-containing medium. [d] Cells were cultivated in lactate-containing medium.

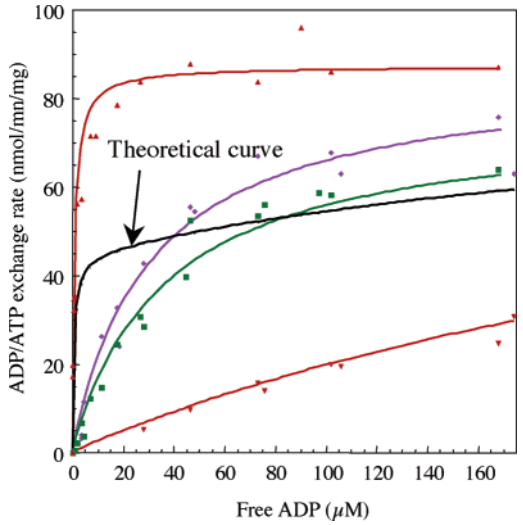

FIGURE 4: Anc2/op1 protomers cooperate during ADP/ATP exchange. The ADP/ATP exchange rate was measured as a function of free ADP concentration (0−900 μM) for mitochondria containing Anc2p (red ▲), Anc2-op1p (green ■), op1-Anc2p (violet ◆), or op1p (red ▼). Data were fitted with the Michaelis−Menten equation. The theoretical curve corresponds to a rate calculation as a function of ADP concentration considering two independent protomers: one with Anc2p kinetic parameters and the other with op1p kinetic parameters.

~3 times the K_M^{ADP} value [compare Anc2p and $(Anc2p)_2$ in Table 3]. The covalent Anc2/op1 chimeras combine both effects, but the effect of op1 is much less dramatic: the K_M^{ADP} values increased only 50−60 times instead of 540 times as observed for the op1p mutant (Table 3). Obviously, the two protomers within a covalent dimer do not function independently.

The exchange rate variation as a function of ADP concentration can be fitted with a hyperbola in every case (Figure 4). We have calculated what this variation would be if the two subunits were functioning independently within Anc2/op1 heterochimeras. As can be seen in Figure 4, such a hypothesis cannot account for the experimental data points obtained for Anc2/op1 heterochimeras. We can therefore conclude that both protomers cooperate during nucleotide exchange, and consequently, this conclusion can be applied to wild-type Anc2p, which was previously postulated to function as a dimer (*6*).

The Anc2/Pic heterochimeras exchanged nucleotides with a V_{max}^{ADP} value similar to that of Anc2p, but the K_M^{ADP} values

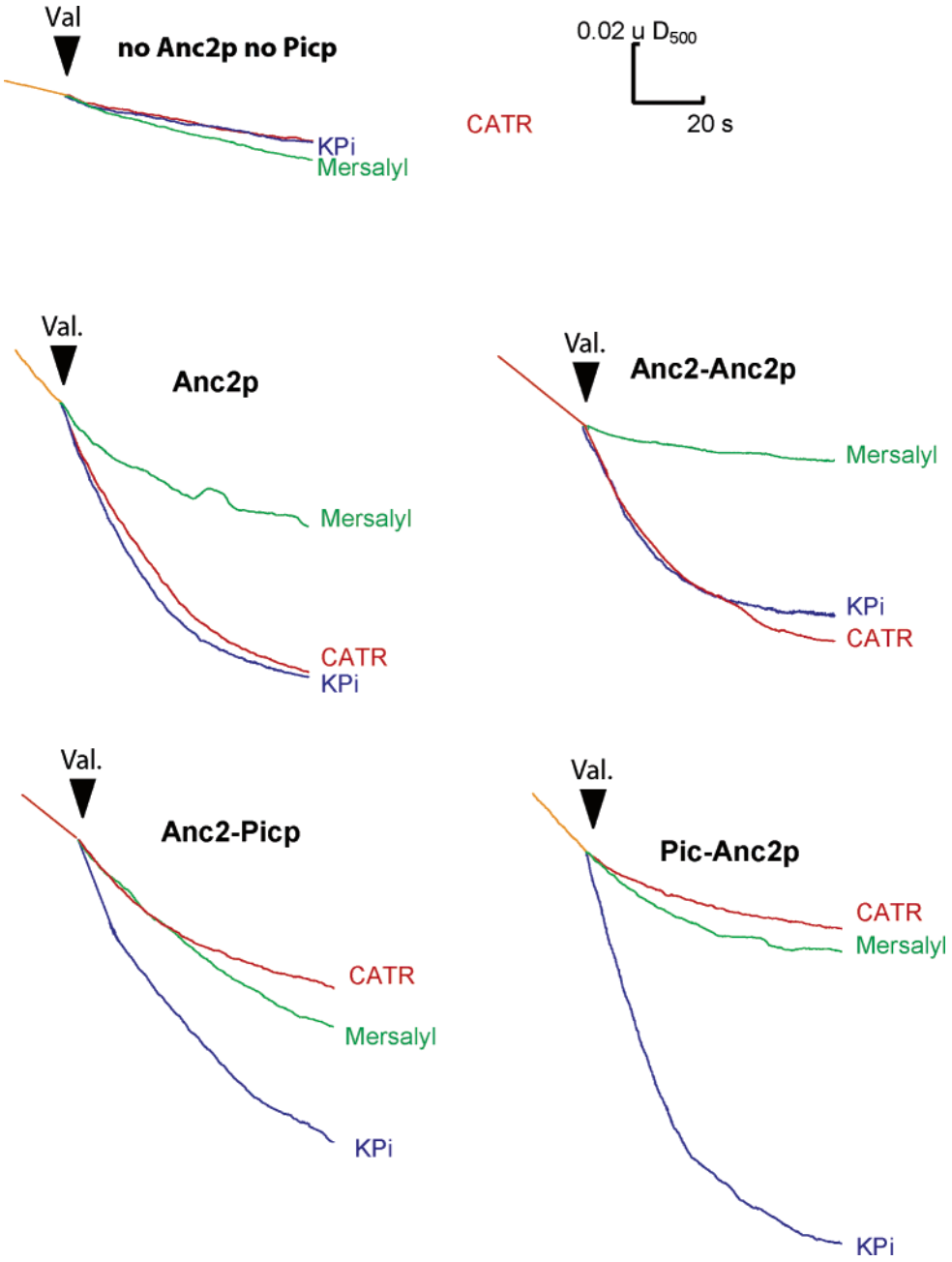

FIGURE 5: Anc2/Pic chimeras are sensitive to inhibitors of both carriers, CATR and mersalyl. Mitochondria were isolated from Δ*anc*Δ*pic* cells or *JL1-3-ANC2* (Anc2p), *JL1-3-(ANC2)*$_2$ [(Anc2p)$_2$], ANC2-op1 (Anc2-op1p), or op1-ANC2 (op1-Anc2p) cells and were incubated (0.2 mg of protein) in 240 mM KP_i (pH 6.8). Swelling is initiated by addition of valinomycin (0.4 μg/mg of proteins) (blue) and monitored as a decrease in the D_{500} of mitochondrial suspensions. Mersalyl is added at a concentration of 125 nmol/mg of proteins (green), and CATR is added at a concentration of 1.25 nmol/mg of proteins (red).

were much closer to that of Anc2p than in the case of the Anc2/op1 chimeras (Table 3). Thus, unlike the op1 protomer, the Pic protomer does not dramatically affect Anc2 protomer function within the heterochimeras.

Anc2/Pic Heterochimeras Are Sensitive to Anc2p and Picp Inhibitors. The rate of P_i uptake can be estimated in vitro by following mitochondrial isoosmotic swelling in phosphate buffers. Movement of phosphate ions across MIM increases mitochondrial osmotic pressure resulting in matrix swelling, the rate of which is sustained by addition of valinomycin (0.4 μg/mg of proteins) in potassium phosphate buffer, and FCCP (1 μM) and antimycin A (2.5 μg/mg of proteins) in ammonium phosphate buffer. Swelling is followed by measuring the attenuance at 500 nm. Its initial rate after valinomycin addition is proportional to the rate of phosphate transport. Whereas Δ*anc2*Δ*pic* mitochondria are unable to swell in KP_i buffer, Anc2p, Anc2-Anc2p mitochondria—which still have the wild-type phosphate carrier—swell in potassium phosphate buffer (Figure 5) as well as in ammonium phosphate buffer (not shown). Whatever the buffer, swelling is sensitive to mersalyl (125 nmol/mg of proteins), a SH reagent inhibiting Picp, and insensitive to 5 μM CATR, a specific Anc2p inhibitor (Figure 5), indicating that CATR has no effect on wild-type Picp. Mitochondria containing Anc2/Pic heterochimeras do no contain wild-type Picp, but interestingly swell in potassium phosphate (Figure 5) or ammonium phosphate buffer (not shown). This swelling is sensitive to mersalyl, indicating that Anc2/Pic heterochimeras

catalyze P_i transport through Pic protomers, but very surprisingly, swelling is also strongly inhibited by 5 μM CATR (Figure 5), indicating that P_i transport inhibition involves in one way or another the Anc2 protomer. Ancp is very specific to ADP and ATP nucleotides, and does not transport P_i. Therefore, CATR inhibition of mitochondrial swelling is very likely an indirect one.

DISCUSSION

Several lines of evidence indicate that mitochondrial carriers function as dimers (*3*, *5*, *7*, *20*, *21*). Those are particularly abundant in the case of the bovine ADP/ATP carrier (*2*−*6*). However, the only three-dimensional (3D) structure of mitochondrial carrier obtained at high resolution shows a monomer organization of the bovine Anc1p (BAnc1p) (*1*). It was suggested that such a monomer organization could result from purification and crystallization processes. Indeed, it is necessary to concentrate the protein at concentrations compatible with crystallization trials, and during this step, the detergent used to make the carrier soluble and purify it is also concentrated. This can lead to a monomerization artifact. The 3D structure was obtained for BAnc1p complexed to CATR. This inhibitor binds almost irreversibly to Ancp and blocks it into a stable conformation, and the calculated binding stoichiometry is 1 mol of CATR per 2 mol of BAnc1p (*2*−*5*).

The topography of Anc2p was investigated by engineering a covalent tandem dimer of Anc2p, the in vivo and in vitro properties of which were quite similar to that of the wild-type carrier (*8*). We concluded the number of TMS was even and in addition if Anc2p was a dimer, the N-ter of one subunit would be close to the C-ter of another subunit within MIM. Such a covalent tandem dimer was an appropriate frame for studying subunit interactions by replacing one of the protomers with an inactive one.

We have chosen to use on one hand an almost inactive mutant of Anc2p, *op1*, which precludes yeast growth on a nonfermentable carbon source. To go one step beyond and take advantage of amino acid sequence conservation between mitochondrial carriers, we have used on the other hand another MCF member, the phosphate carrier (Picp). Our choice was dictated by the work by Schroers et al. (*7*), who showed that Picp dimerization is a prerequisite for in vitro function. Indeed, Picp activity depended on the lipid environment and on the detergents used for isolation and reconstitution. When isolated in the presence of sodium lauroyl sarcosinate and *n*-dodecyl octaethylene glycol monoether, Picp was inactive, and a higher degree of organization was necessary to achieve phosphate uptake in a reconstituted system. Furthermore, crosstalk between subunits was mandatory for Picp activity since co-reconstitution of active and inactive subunits precluded in vitro phosphate uptake (*7*).

Crosstalk between Anc2p subunits was not as obvious because Anc2/op1 chimera genes could confer efficient growth on nonfermentable carbon sources of *JL1-3Δ2* cells, of which the endogenous *ANC* genes were initially inactivated. At this stage of the work, we could not exclude the possibility that growth was restored by wild-type Anc2p, resulting from proteolytic cleavage of the chimeras. Indeed, during our former studies of the covalent tandem dimer of Anc2p, we were confronted by its sensitivity to proteolytic cleavage that generated a band migrating at the position of the Anc2p monomer on SDS−PAGE (*8*). Addition of a cocktail of antiproteases prevented the appearance of this band. Therefore, the covalent link between two Anc2 protomers exposed to proteolytic cleavage the region encompassing the C-ter of one protomer and the N-ter of the second protomer. Yeast Anc2p and Banc1p sequences are 48.3% identical, and therefore, an analogy can be drawn between the known BAnc1p 3D structure (*1*) and the unknown ScAnc2p structure. We can thus estimate that for ScAnc2p, the hydrophilic N-ter and C-ter regions exposed toward the cytosol would be 17 and 12 amino acids long, respectively. In the covalent tandem dimer $(Anc2p)_2$, the peptide connecting TMS 6 of one protomer to TMS 1 of the second protomer would be 29 amino acids long and would probably be unstructured. This could account for the sensitivity of this region to proteolytic degradation. As a matter of fact, we could exclude the possibility that Anc2/op1 covalent heterodimers were proteolyzed from immunodecoration experiments (Figure 1A). Thus, growth on nonfermentable carbon sources was restored by full-size Anc2/op1 chimeras. They are therefore active to exchange adenine nucleotides.

A piece of evidence of crosstalk between Anc2p monomers came from analyses of ADP/ATP exchange rate variation as a function of ADP concentration (Figure 4). K_M^{ADP} values for Anc2/op1 chimeras were intermediate between that of wild-type Anc2p and those of op1p and op1-op1p variants (Table 3). Besides, we have calculated what the variation of the V^{ADP} value as a function of ADP concentration would be if the two protomers were functioning independently. It would be the sum of half of the activities of each of the noncovalent dimers, ScAnc2p (WT) and op1p, following eq 1:

$$V^{ADP} = {}^1/_2[[ADP]V_{max}{}^{WT}/(K_M{}^{WT} + [ADP])] + {}^1/_2[[ADP]V_{max}{}^{op1}/(K_M{}^{op1} + [ADP])] \quad (1)$$

The theoretical resulting graph, in which $V^{ADP} = f([ADP])$, is quite different from the experimental ones obtained for the Anc2/op1 heterochimeras (Figure 4), and the difference is too important for experimental variations to account for. This establishes the existence of crosstalk between protomers of Anc2/op1 chimeras, though its nature is unknown for the time being. A negative effect of the op1 protomer on Anc2 protomer insertion within MIM, and putatively on the exchange activity of the heterochimeras, was ruled out by limited proteolysis experiments that evidenced that both protomers were digested similarly under mild conditions (Figure 3). We could conclude that they were folded similarly in the membrane, thus exposing the same peptidic regions to proteolysis. Therefore, kinetic properties of Anc2/op1 chimeras reflect cooperation between protomers during nucleotide exchange, and very likely between monomers of wild-type Anc2p. One explanation lies in the exchange mechanism that is a strict exchange of one nucleotide taken from one side of the mitochondrial membrane for one nucleotide taken from the other side. One can imagine that during the catalytic cycle, the exchange could be achieved only when both monomers of the dimer bound nucleotides but from the opposite sides of the membrane. A strong

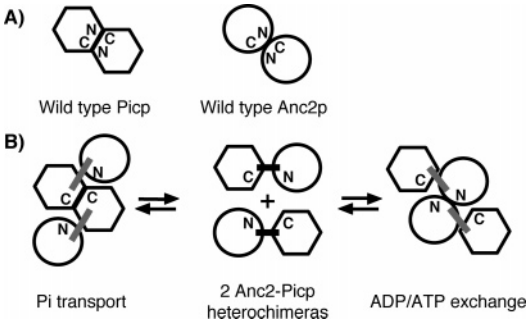

FIGURE 6: Dimerization of Anc2/Pic heterochimeras. (A) In the wild-type Anc2p and Pic carriers, the contact regions between monomers are between TMS 1 and 6, as suggested from studies described in ref *8*. B) Covalent Anc2/Pic heterochimeras (middle) interact to form pseudotetramers competent for either P_i transport (left) or ADP/ATP transport (right). The black line stands for the covalent link between Anc2 and Pic protomers (middle). It is colored in gray to account for movements of the protomers to form the pseudotetramers (left and right).

positive cooperativity in substrate binding was postulated in the case of rat heart Ancp (*6*) but cannot be deduced from our experiments with yeast Anc2p.

Unlike Anc2/op1 chimeras, Anc2/Pic chimeras exhibit nucleotide exchange activities similar to that of wild-type Anc2p. This was unexpected since we had concluded from Anc2/op1 chimera kinetic properties that both protomers were cooperating to perform nucleotide exchange. Such a behavior of Anc2/Pic chimeras would be consistent with the hypothesis of a monomeric functional unit of Anc2p. However, dimerization is a prerequisite for Picp function, as demonstrated in ref *7*, and Ancp very likely functions as a dimer (*6*). Therefore, one can imagine that two Anc2/Pic chimeras associate in a pseudotetramer to build up an active Pic carrier from two interacting Pic protomers or an active Anc2 carrier from two interacting Anc2 protomers, as illustrated in Figure 6. In Figure 6B, we have considered that the interfaces between two identical protomers of two distinct covalent heterochimeras were the same as that between two monomers in the noncovalent wild-type dimers (Figure 6A). Therefore, both activities (ADP/ATP and P_i transports) cannot coexist within the same pseudotetramer molecule. This implies that the protomers in a covalent heterochimera can move apart to reconstitute an active carrier, of the Pic or Anc2 type, which thus exhibits kinetic properties similar to that of the wild-type carrier, Picp or Anc2p. The fact that CATR, a very specific inhibitor of Anc2p, inhibited phosphate uptake only in the case of Anc2/Pic chimeras and not in the case of Picp or Anc2-Anc2p (Figure 5) reinforces this hypothesis. When CATR binds, two Anc2 protomers of two different heterochimeras move closer together and the Pic protomers move apart, precluding phosphate transport activity.

One can imagine two alternatives to explain that Anc2/Pic chimeras restore both nucleotide and P_i transports: either one dimer of Anc2/Pic chimeras (a pseudo-tetramer) can catalyze both transports, or two types of pseudotetramers coexist in the cell (Figure 6). One would transport ADP and ATP and the other Pic. A full inhibition of swelling in the presence of CATR (Figure 5) is consistent with the hypothesis of an interconversion between two pseudotetramer forms (Figure 6B), ruling out the possibility that the same pseudotetramer can catalyze simultaneously P_i and ADP/ATP transport. The two types of pseudotetramers would be in equilibrium so that CATR binding would displace this equilibrium toward the "Anc2p competent" conformation (Figure 6B, right side). In vivo, dimer formation (stage V) follows monomer insertion of wild-type Anc2p (stage IV) and is a rapid stage (less than 1 min in vitro) (*22*). The incoming monomer would dimerize with endogenous Anc2p monomers, suggesting that the Ancp dimer is very dynamic (*22*) and thus supporting an efficient interconversion between Anc2/Pic pseudotetramers.

Covalent tandem dimers of Ancp are also of potential use in delineating the dimerization interface of Anc2p. For this purpose, after induction of inactive mutants of Anc2p by UV or chemical mutagenesis, their dominance or recessiveness would be assayed within the frame of covalent heterodimer constructs similar to the op1/Anc2 ones. The op1 protomer would be replaced with an inactive mutant protomer. Indeed, dominant mutations are very likely to change residues involved in dimerization. Dimer formation could thereafter be assessed by blue native PAGE.

ACKNOWLEDGMENT

We are grateful to Claudine David for her technical assistance.

REFERENCES

1. Pebay-Peyroula, E., Dahout-Gonzalez, C., Kahn, R., Trézéguet, V., Lauquin, G. J.-M., and Brandolin, G. (2003) Structure of mitochondrial ADP/ATP carrier in complex with carboxyatractyloside, *Nature 426*, 39−44.
2. Riccio, P., Aquila, H., and Klingenberg, M. (1975) Purification of the carboxy-atractylate binding protein from mitochondria, *FEBS Lett. 56*, 133−8.
3. Klingenberg, M., Riccio, P., and Aquila, H. (1978) Isolation of the ADP, ATP carrier as the carboxyatractylate·protein complex from mitochondria, *Biochim. Biophys. Acta 503*, 193−210.
4. Hackenberg, H., and Klingenberg, M. (1980) Related molecular weight and hydrodynamic parameters of the adenosine 5′-diphosphate-adenosine 5′-triphosphate carrier in Triton X-100, *Biochemistry 19*, 548−55.
5. Block, M. R., Zaccaï, G., Lauquin, G. J.-M., and Vignais, P. V. (1982) Small angle neutron scattering of the mitochondrial ADP/ATP carrier protein in detergent, *Biochem. Biophys. Res. Commun. 109*, 471−7.
6. Duyckaerts, C., Sluse-Goffart, C. M., Fux, J. P., Sluse, F. E., and Liebecq, C. (1980) Kinetic mechanism of the exchanges catalysed by the adenine-nucleotide carrier, *Eur. J. Biochem. 106*, 1−6.
7. Schroers, A., Burkovski, A., Wohlrab, H., and Kramer, R. (1998) The phosphate carrier from yeast mitochondria. Dimerization is a prerequisite for function, *J. Biol. Chem. 273*, 14269−76.
8. Trézéguet, V., Le Saux, A., David, C., Gourdet, C., Fiore, C., Dianoux, A., Brandolin, G., and Lauquin, G. J.-M. (2000) A covalent tandem dimer of the mitochondrial ADP/ATP carrier is functional in vivo, *Biochim. Biophys. Acta 1757*, 81−93.
9. Kováč, L., Lachowicz, T. M., and Slonimski, P. P. (1967) Biochemical genetics of oxidative phosphorylation, *Science 158*, 1564−7.
10. Kolarov, J., Kolarova, N., and Nelson, N. (1990) A third ADP/ATP translocator gene in yeast, *J. Biol. Chem. 265*, 12711−6.
11. Gawaz, M., Douglas, M. G., and Klingenberg, M. (1990) Structure−function studies of adenine nucleotide transport in mitochondria. II. Biochemical analysis of distinct AAC1 and AAC2 proteins in yeast, *J. Biol. Chem. 265*, 14202−8.
12. Müller, V., Basset, G., Nelson, D. R., and Klingenberg, M. (1996) Probing the role of positive residues in the ADP/ATP carrier from yeast. The effect of six arginine mutations on oxidative phosphorylation and AAC expression, *Biochemistry 35*, 16132−43.
13. Dietmeier, K., Zara, V., Palmisano, A., Palmieri, F., Voos, W., Schlossmann, J., Moczko, M., Kispal, G., and Pfanner, N. (1993) Targeting and translocation of the phosphate carrier/p32 to the

inner membrane of yeast mitochondria, *J. Biol. Chem. 268*, 25958−64.
14. Drgoň, T., Šabová, L., Nelson, N., and Kolarov, J. (1991) ADP/ATP translocator is essential only for anaerobic growth of yeast *Saccharomyces cerevisiae*, *FEBS Lett. 289*, 159−62.
15. De Marcos Lousa, C., Trézéguet, V., Dianoux, A.-C., Brandolin, G., and Lauquin, G. J.-M. (2002) The human mitochondrial ADP/ATP carriers: Kinetic properties and biogenesis of wild type and mutant proteins in the yeast *S. cerevisiae*, *Biochemistry 41*, 14412−20.
16. Brandolin, G., Le Saux, A., Trézéguet, V., Vignais, P. V., and Lauquin, G. J.-M. (1993) Biochemical characterisation of the isolated Anc2 adenine nucleotide carrier from *Saccharomyces cerevisiae* mitochondria, *Biochem. Biophys. Res. Commun. 192*, 143−50.
17. Brandolin, G., Meyer, C., Defaye, G., Vignais, P. M., and Vignais, P. V. (1974) Partial purification of an atractyloside-binding protein from mitochondria, *FEBS Lett. 46*, 149−53.
18. Sikorski, R. S., and Hieter, P. (1989) A system of shuttle vectors and yeast host strains designed for efficient manipulation of DNA in *Saccharomyces cerevisiae*, *Genetics 122*, 19−27.
19. Le Saux, A., Roux, P., Trézéguet, V., Fiore, C., Schwimmer, C., Dianoux, A.-C., Vignais, P. V., Brandolin, G., and Lauquin, G. J.-M. (1996) Conformational changes of the yeast mitochondrial adenosine diphosphate/adenosine triphosphate carrier studied through its intrinsic fluorescence. 1. Tryptophanyl residues of the carrier can be mutated without impairing protein activity, *Biochemistry 35*, 16116−24.
20. Lin, C. S., Hackenberg, H., and Klingenberg, M. (1980) The uncoupling protein from brown adipose tissue mitochondria is a dimer. A hydrodynamic study, *FEBS Lett. 113*, 304−6.
21. Klingenberg, M. (1981) Membrane oligomeric structure and transport function, *Nature 290*, 449−54.
22. Dyall, S. D., Agius, A. C., De Marcos Lousa, C., Trézéguet, V., and Tokatlidis, K. (2003) The dynamic dimerization of the yeast ADP/ATP carrier in the inner mitochondrial membrane is affected by conserved cysteine residues, *J. Biol. Chem. 278*, 26757−64.

BI051648X